

1 **Assessing bacterial infiltration through reverse osmosis**
2 **membrane**

3 Takahiro Fujioka* and Sandrine Boivin

4 *Graduate School of Engineering, Nagasaki University,*
5 *1-14 Bunkyo-machi, Nagasaki 852-8521, Japan*

6
7

8 * Corresponding author: Takahiro Fujioka, Email: tfujioka@nagasaki-u.ac.jp, Tel: +81 095 819 2695, Fax:
+81 95 819 2620

9 **Abstract**

10 The attenuation of pathogenic microorganisms in potable water reuse is critical to ensure
11 recycled water safety. Thus, this study sought to identify bacterial communities capable of
12 passing through a commercial reverse osmosis (RO) membrane as well as to characterize the
13 passage of these bacteria through the membranes. Three-quarters of the bacteria in the RO
14 permeate were found to belong to the Burkholderiaceae family, although this family only
15 accounted for 0.2% of the RO feed (i.e., ultrafiltration-treated wastewater) bacterial
16 composition. The infiltration routes of bacteria through the RO membranes was also
17 evaluated using a unique approach—capturing bacteria-sized surrogates (i.e., 0.5 μm
18 fluorescent (FL) microspheres) with a track-etched micro-filter after passing through the RO
19 membrane. Our results demonstrated that a considerable number of FL particles passed
20 through the membranes that were obtained from an RO membrane element. Overall, it was
21 determined that certain bacterial families in wastewater could pass through the passage
22 located in the entire surface of the RO membrane rather than in localized areas. Thus, this
23 study highlights the need to reinforce RO membrane integrity in order to ensure the safety of
24 recycled water for potable water reuse.

25 **Keywords:** Bacterial removal; membrane integrity; RO membrane; gene sequencing; potable
26 water reuse.

27

28 1 Introduction

29 Pathogen control in potable water reuse is a critical public health measure (Pecson et al.,
30 2017). Potable water reuse is accomplished by converting conventionally treated wastewater
31 (i.e., secondary wastewater effluents) to highly purified drinking water. Thus, the attenuation
32 of pathogenic microorganisms (e.g., virus, protozoa, and bacteria) through advanced
33 wastewater treatment is critical. Advanced wastewater treatment systems encompass multiple
34 barriers and treatment procedures such as microfiltration (MF) or ultrafiltration (UF), reverse
35 osmosis (RO) membranes, advanced oxidation processes (AOP), and chlorine disinfection
36 (Fujioka et al., 2012). Furthermore, the attenuation of pathogens in potable water reuse can be
37 quantitatively managed by implementing a log reduction credit approach. For instance,
38 California (USA) requires advanced wastewater treatment systems to meet a reduction value
39 of 12-log, 10-log, and 10-log for virus, *Cryptosporidium*, and *Giardia*, respectively. Further,
40 a 9-log reduction target has been suggested for total coliform bacteria for direct potable water
41 reuse (NWRI, 2013).

42 Among advanced wastewater treatment processes, the RO membrane treatment has been
43 undervalued with as little as a 2.0-log reduction credit value based on conservative surrogate
44 indicators (e.g., electrical conductivity removal, which achieves up to 99% removal) that
45 have widely been used to monitor and ensure RO membrane integrity (Tchobanoglous, 2015;
46 WHO, 2017). Increasing the log reduction value of RO membranes could reduce the
47 dependence on other bacterial removal processes, including AOP. For instance, recent
48 advances in analytical technology (e.g. real-time bacteriological counters) could allow for
49 continuous bacterial attenuation monitoring, thus potentially increasing the log reduction
50 credit value for RO membranes (Fujioka et al., 2018b; Fujioka et al., 2019b).

51 In addition to improved monitoring techniques, the reliability of RO treatment for effective
52 bacterial removal is also critical. To date, RO membrane reliability has been evaluated via
53 integrity breaches caused by intentionally damaging the RO membrane (e.g., by creating
54 pinholes on their surface) or the pressure vessel components (e.g., O-rings) (Antony et al.,
55 2012; Kitis, Mehmet et al., 2003; Kitis, M. et al., 2003; Mi et al., 2004; Pype et al., 2016;
56 Zhang et al., 2016). However, bacterial passage through intact (i.e., undamaged) RO
57 membrane elements has been seldom addressed. Bacterial size (i.e., typically $> 0.2 \mu\text{m}$) is
58 three orders of magnitude greater than the free-volume hole size of RO membranes (< 0.001
59 μm) (Fujioka et al., 2018c), meaning that in theory all bacteria should be rejected by RO
60 membranes. However, many studies have identified high concentrations of bacteria in pilot-
61 and full-scale RO system permeates (Ishida and Cooper, 2015; Kantor et al., 2019; Laurent et
62 al., 1999; Liikanen et al., 2003; Miller et al., 2017; Park and Hu, 2010), indicating that RO is
63 not an infallible barrier against bacteria. A recent study (Fujioka and Boivin, 2019) also
64 confirmed the passage of particles through RO membranes using $0.5 \mu\text{m}$ fluorescent (FL)
65 microspheres, which are surrogates similarly-sized to bacteria (e.g., *Escherichia coli* that has
66 a diameter of $0.5 \mu\text{m}$ and a length of $2 \mu\text{m}$).

67 A better understanding of bacterial passage through RO membranes could potentially lead to
68 enhanced bacterial removal and improve the reliability of RO membranes. Our previous
69 study (Fujioka et al., 2019a) found that bacteria could pass through intact O-ring seals, which
70 connect multiple RO membrane elements and pressure vessel end caps. Our study also found
71 that bacteria-sized surrogates (i.e., fluorescent microspheres) passed through different types
72 of 4-inch RO membrane elements even after bonding the O-ring seals between the RO
73 membrane element and the pressure vessel end-ports, indicating that bacterial passage can
74 occur through the RO membranes themselves. Another recent study (Fujioka and Boivin,
75 2019) found that the integrity of RO membrane sheets for bacterial removal could be

76 compromised during their assembly processes. However, the previous study did not identify
77 the bacterial communities that were passing through, nor did it explain how they passed
78 through the RO membrane.

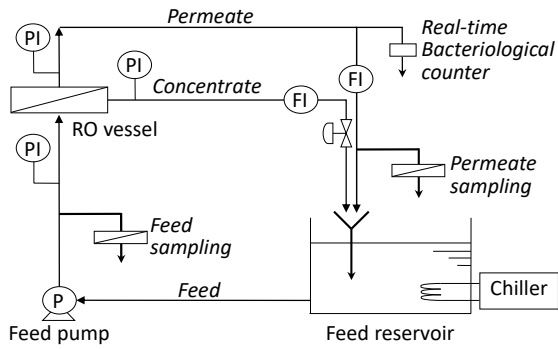
79 Therefore, the present study sought to identify bacterial communities that pass through RO
80 membranes as well as their infiltration routes. Bacteria in RO feed and permeate were
81 identified via bacterial cell counts by fluorescent staining and fluorescence microscopy, and
82 16S rRNA gene sequencing. In addition, their infiltration routes were evaluated using a
83 unique approach—capturing bacteria-sized surrogates (i.e., 0.5 μm fluorescent microspheres)
84 with a track-etched micro-filter after passing through the RO membrane.

85 **2 Materials and methods**

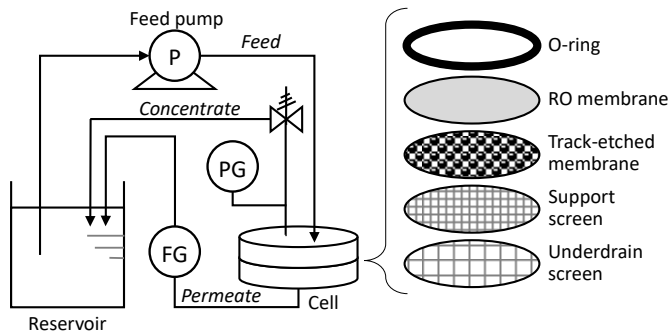
86 ***2.1 Membranes and treatment systems***

87 **2.1.1 Pilot-scale system**

88 Bacterial infiltration through RO membranes was evaluated using a 4-inch spiral-wound
89 polyamide (PA) composite RO membrane element (ESPA2-LD-4040, Hydranautics;
90 Oceanside, CA, USA). The pilot-scale cross-flow RO system (**Fig. 1a**) consisted of a 4-inch
91 end-port fiberglass pressure vessel (40E30N, Codeline/Pentair Water; Goa, India), a 65-L
92 stainless steel reservoir, a high-pressure pump (25NED15Z, Nikuni Co., Ltd.; Kawasaki,
93 Japan), digital flow indicators (FDM, Keyence Co.; Osaka, Japan), digital pressure indicators
94 (GPM, Keyence Co.; Osaka, Japan), and a chiller unit (CA-1116A, Tokyo Rikakikai Co.
95 Ltd.; Tokyo, Japan). The O-ring seal between the RO membrane element and the pressure
96 vessel end-ports was bonded with adhesives to prevent bacteria from passing through the seal.



97
98 (a) Pilot-scale cross-flow RO system



99
100 (b) Bench-scale cross-flow RO system

101 **Fig. 1** Diagrams of the (a) pilot-scale and (b) bench-scale RO treatment systems.

102 **2.1.2 Bench-scale system**

103 The location in the RO membrane sheets where bacterial passage occurred was examined in
 104 bench-scale experiments. Two different RO membrane conditions were examined herein: (a)
 105 RO membrane sheets without undergoing an RO element assembly process (i.e., hereafter
 106 referred to as “intact RO”) and (b) RO membrane sheets after disassembling the RO element
 107 (i.e., hereafter referred to as “disassembled RO”). Previously inspected and certified
 108 polyamide composite RO membrane samples were supplied by an RO membrane
 109 manufacturer. Disassembled RO membrane samples were prepared by dismantling two RO
 110 membrane elements that had satisfied the manufacturer's specified performance. The bench-
 111 scale cross-flow RO system (**Fig. 1b**) was comprised of a 47-mm cross-flow stainless steel
 112 filter holder (XX440470, Merck; Tokyo, Japan), a dual plunger pump (KP-22, FLOM; Tokyo,
 113 Japan), a flow gauge, a pressure indicator, and a chiller unit (ACE-1100, Tokyo Rikakikai Co.
 114 Ltd.; Tokyo, Japan) (**Fig. 1a**). To capture all particles passing through the RO membrane, a

115 track-etched polycarbonate MF filter with a uniform pore size of 0.2 μm (Merck; Tokyo,
116 Japan) was placed between the RO membrane and the support screen (i.e., permeate spacer).

117 **2.2 *Experimental protocol***

118 **2.2.1 Pilot-scale system**

119 A pilot-scale test was conducted with 50 L of UF-treated wastewater, which was prepared by
120 filtering a secondary wastewater effluent with a UF membrane module (SFP-2860XP, Dow
121 Chemical; Midland, MI, USA). The UF membrane module had a membrane surface area of
122 51 m^2 and a nominal pore size of 0.03 μm . Secondary wastewater effluents (3.05 mS/cm
123 conductivity) were collected from a wastewater treatment plant that implemented primary
124 settling and activated sludge. Before testing, the pilot-scale RO system outflow was
125 disinfected using a commercial sterilant especially designed for such purpose (Minicare
126 Sterilant, Mar Cor Purification; Plymouth, MN, USA). Afterward, filtered tap water was
127 recirculated through the system for >12 hours until the RO treatment condition was stable.
128 Then, the water was replaced with the 50 L of UF-treated wastewater. The RO system was
129 then operated at a permeate flux of 16 $\text{L/m}^2\text{h}$, an feed temperature of 25 ± 0.5 $^\circ\text{C}$, and a 14%
130 recovery (permeate and concentrate flow rate = 2.0 and 10 L/minute, respectively) for 27 h.
131 Both the RO permeate and concentrate were recirculated to the feed reservoir. RO feed and
132 permeate samples were periodically collected in a sterile polypropylene bottle and underwent
133 bacterial analysis soon thereafter. Additionally, RO feed and permeate conductivity was
134 analyzed using Orion Star™ A322 Conductivity meters (Thermo Fisher Scientific; Waltham,
135 MA, USA). Bacterial biomass for 16S rRNA gene sequencing was collected from the RO
136 feed and permeate by filtering the samples with a track-etched polycarbonate MF filter (0.2
137 μm pore size; Merck, Tokyo, Japan) at a flow rate of 2 and 150–200 mL/min , respectively.

138 **2.2.2 Bench-scale system**

139 Bench-scale tests were conducted using a stable fluorescent particle (FL; 0.50 μm diameter,
140 diameter variation coefficient = 3%) solution containing Fluoresbrite[®] Yellow Green
141 Carboxylate Microspheres (Polysciences, Inc.; Warrington, PA, USA). These stable FL
142 particles were used as surrogates, as bacteria may occur on the intact RO membrane sheets
143 and become the source of bacterial contamination. The FL solution was mixed into a 10 mM
144 NaCl matrix. Before each test, the RO membrane was compacted to stabilize its performance
145 by treating pure water at 0.6 MPa. Afterward, the water was replaced with 500 mL of
146 solution containing 10 mM NaCl, and the pressure was reestablished to 0.6 MPa. Further, the
147 FL stock solution was added to the RO feed solution at the concentration of approximately
148 2.2×10^7 particles/mL. The system was then operated at a constant permeate flux of 22 L/m²h,
149 a feed flow rate of 40 mL/min, and a feed temperature of 25 °C for 120 min. Following the
150 filtration test, the track-etched polycarbonate MF membrane placed underneath the RO
151 membrane was carefully removed and underwent fluorescence microscopy.

152 **2.3 Analytical protocols**

153 **2.3.1 Bacterial counts**

154 Intact and damaged bacterial counts were determined using a fluorescence microscope (BZ-
155 X800, Keyence Co.; Osaka, Japan). Each 1-mL sample was stained with the LIVE/DEAD
156 BacLight Bacterial Viability Kit (Thermo Fisher Scientific; Waltham, MA, USA) for 15
157 minutes in the dark at room temperature (i.e., approximately 23 °C). The staining kit
158 contained two dyes: SYTO[®]9 and propidium. Afterward, 200 μL of the stained sample was
159 passed through a 0.2 μm pore size track-etched polycarbonate MF filter (Merck; Tokyo,
160 Japan) and analyzed using a green filter (excitation wavelength = 470 ± 40 nm, absorption

161 wavelength = 525 ± 50 nm) and a red filter (excitation wavelength = 545 ± 25 nm, absorption
162 wavelength = 605 ± 70 nm).

163 Bacterial counts in RO permeate were also monitored using a real-time bacteriological
164 counter (IMD-WTM, Azbil Corporation, Tokyo, Japan). The real-time bacteriological counter
165 is capable of counting bacterial particles in real time by measuring the intensity of scattered
166 and fluorescent light that occur in response to the excitation light with a wavelength of 405
167 nm. Details of the instrument are provided elsewhere (Fujioka et al., 2018a).

168 **2.3.2 Bacterial community analysis**

169 Bacterial community analysis with 16S rRNA gene sequencing was conducted at Hokkaido
170 System Science (Sapporo, Japan). Genomic DNA was extracted from the RO feed and
171 permeate biomass samples using the Extrap Soil DNA Kit Plus ver.2 (Nippon Steel Eco-Tech
172 Corporation; Tokyo, Japan). Using the extracted DNA samples, a first-stage PCR
173 amplification of 16S rRNA genes was performed following the 16S Metagenomic
174 Sequencing Library Preparation protocol provided by Illumina K.K. (Tokyo, Japan). The
175 forward and reverse 16S rRNA amplicon polymerase chain reaction (PCR) primer pair used
176 in this study were 341F (5'- TCG TCG GCA GCG TCA GAT GTG TAT AAG AGA CAG
177 CCT ACG GGN GGC WGC AG) and 805R (5'- GTC TCG TGG GCT CGG AGA TGT
178 GTA TAA GAG ACA GGA CTA CHV GGG TAT CTA ATC C), respectively. The
179 amplified products were then purified using AMPure XP beads, after which a second PCR
180 (i.e., indexed PCR) was performed with dual indices and Illumina sequencing adapters using
181 the Nextera XT Index Kit. The purification of the final library was performed with AMPure
182 XP beads. The products were then sequenced (paired-end, 300 bp) using the MiSeq platform
183 (Illumina K.K., Tokyo, Japan). The resulting sequences were initially processed by base
184 calling, filtering, and trimming of each sequence to yield high-quality reads. Afterward,

185 sequence assembly and cluster generation were performed to create OTUs (i.e., operational
186 taxonomic units). The QIIME (v1.8.0) bioinformatics pipeline was used for cluster generation.
187 Analysis of the bacterial community was conducted for each OTU by searching homology in
188 the 16S rRNA gene sequence database (Greengenes v13.8).

189 **2.3.3 Membrane characterizations**

190 FL particles that passed through RO membranes and deposited on the track-etched MF filter
191 with a diameter of 47 mm were analyzed using a fluorescence microscope (BZ-X800,
192 Keyence Co.; Osaka, Japan). The filter area was analyzed using a green filter as indicated
193 above, but without the addition of stains. A 118 mm² (11.6 × 10.2 mm) area at the center of
194 each filter was examined. FL particle counts were also determined automatically with
195 specialized software (BZ-X800 Analyser, Keyence Co.; Osaka, Japan). Field emission -
196 scanning electron microscope (FE-SEM) (S-4800, Hitachi, Japan) was used to obtain a cross-
197 sectional image of ESPA2 RO membrane. Prior to the analysis, a membrane sample
198 underwent freeze-fracturing, air drying, and coating with conductive material (Fujioka et al.,
199 2018c).

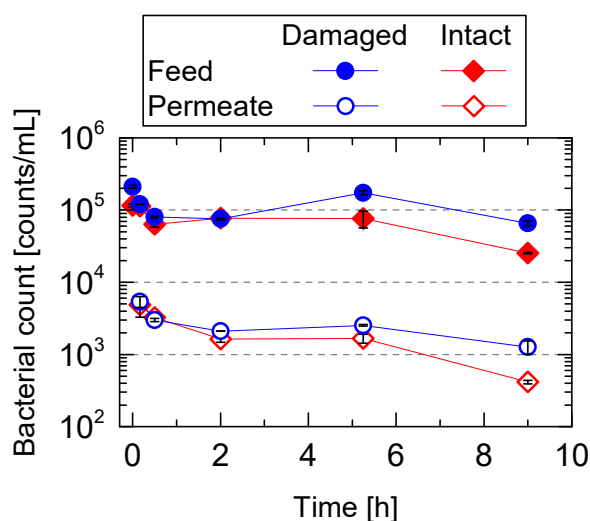
200 **3 Results**

201 ***3.1 Passage through an RO element***

202 **3.1.1 Bacterial counts**

203 Bacterial passage through the RO membrane element was quantitatively evaluated with
204 manually stained and counted bacteria using fluorescence microscopy (i.e., intact and
205 damaged bacterial counts). The UF-treated wastewater used in this study contained high
206 bacterial concentrations of > 10⁵ counts/mL (**Fig. 2**). It is noted that although bacterial counts
207 determined by heterotrophic plate counting method in RO feed (i.e., counts of colony-

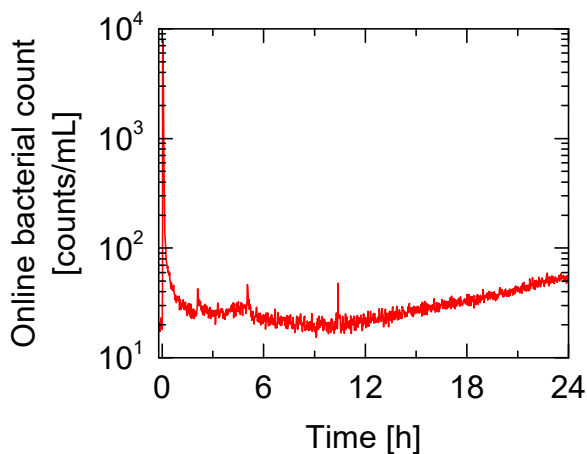
208 forming bacteria) are typically found at < 100 CFU/mL, high concentrations of total bacterial
 209 cells determined by fluorescent staining in RO feed (e.g., 10^3 – 10^6 counts/mL) have been
 210 reported during pilot- or full-scale studies (Ishida and Cooper, 2015; Kantor et al., 2019;
 211 Miller et al., 2020). Thus, the UF-treated wastewater used in this study was not unusual. Pore
 212 size of the UF membrane element of this study ($0.03\ \mu\text{m}$) was considerably smaller than
 213 typical bacterial size ($> 0.2\ \mu\text{m}$). However, UF membrane element with a large membrane
 214 surface area has a potential of lesser membrane integrity than a small membrane samples that
 215 are typically at bench scale; thus, the log reduction of bacteria or bacteria-sized particles by
 216 UF membrane elements can range between 2 and 3-log (Hagen, 1998; Jacangelo et al., 1989).



217
 218 **Fig. 2** Intact and damaged bacterial counts in the RO feed and permeate (transmembrane
 219 pressure of 270 kPa, permeate flux of $16\ \text{L}/\text{m}^2\text{h}$, feed temperature of $25 \pm 0.5\ ^\circ\text{C}$, and system
 220 recovery of 14%). The symbols and error bars of bacterial counts represent the average and
 221 ranges of duplicated analysis samples.

222 Throughout the pilot-scale RO treatment, the numbers of both intact and damaged bacteria in
 223 the RO feed and permeate gradually decreased (**Fig. 2**). Bacterial removal value after 5 h
 224 were 1.7–1.8-log (i.e., 98% removal), which was similar to the conductivity rejection during
 225 the test (98.2–98.5%). It should be noted that the RO system was operated at a permeate flux
 226 of $16\ \text{L}/\text{m}^2\text{h}$, which was slightly lower than a typical permeate flux ($20\ \text{L}/\text{m}^2\text{h}$), and a higher

227 permeate flux can enhance the rejection of constituents including salts (Wijmans and Baker,
228 1995). A recent pilot-scale study (Miller et al., 2020) also reported that nanofiltration and RO
229 membranes achieved low bacterial removal values (1.7–1.8-log) when bacterial cells were
230 counted based on fluorescent staining and flow cytometry. This indicated that approximately
231 2% of bacterial cells in the RO feed were continuously passing through the RO membrane
232 regardless of whether they were intact or damaged. It is noted that high concentrations of
233 bacteria in the RO permeate was detected during the first 30 min after changing water matrix
234 (i.e. from pure water to UF-treated wastewater) (**Fig. 3**). The online bacterial counting results
235 also confirmed the reduction in bacterial counts determined by epifluorescence microscopy
236 and continuous passage of bacteria through the RO membrane element.

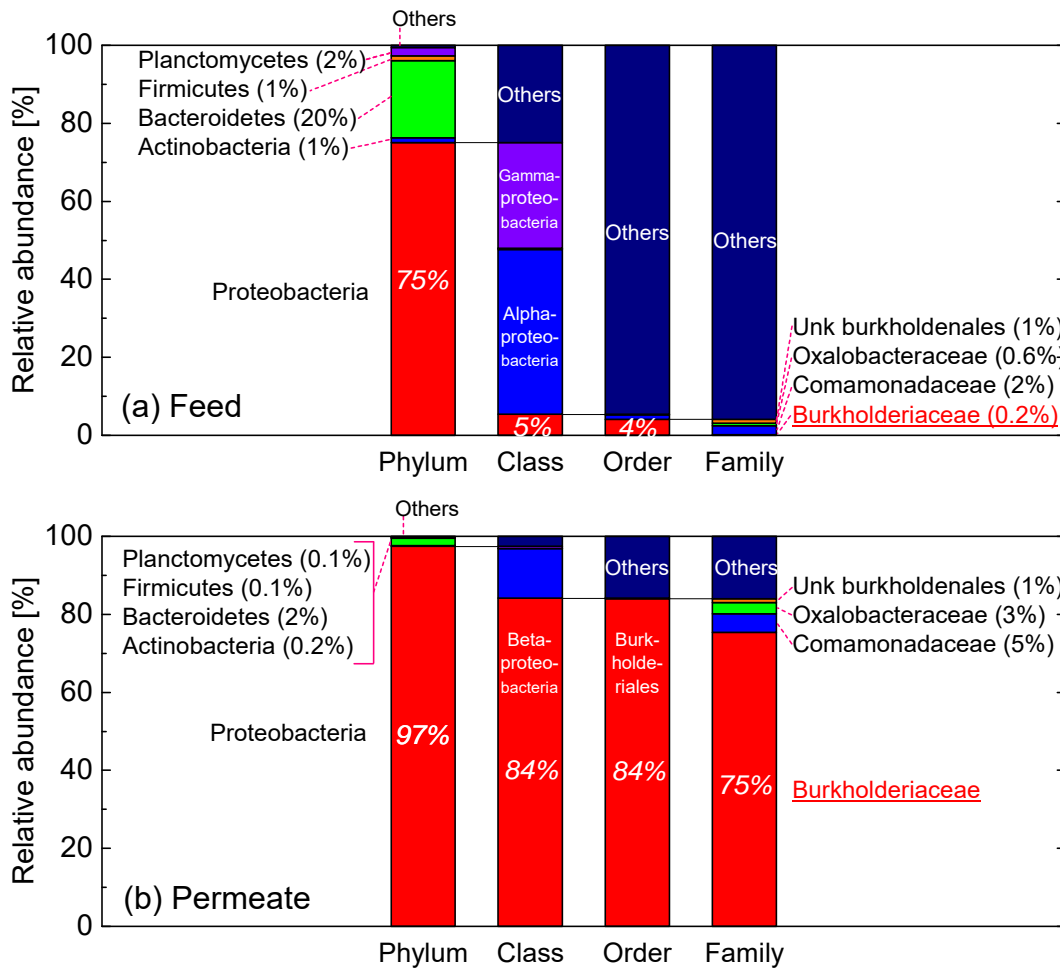


237
238 **Fig. 3** Bacterial counts in the RO permeate that were online monitored using a real-time
239 bacteriological counter during the pilot-scale test (flow rate of 10 mL/min).

240 3.1.2 Bacterial communities

241 Bacterial communities in both the RO input and permeate of the pilot-scale system were
242 analyzed. Proteobacteria was found to be the major phylum (75%; **Fig. 4a**) in the RO feed,
243 whereas it accounted for 97% of bacteria in the RO permeate (**Fig. 4b**); compared to other
244 phyla, Proteobacteria were the least affected by RO treatment. Proteobacteria have been
245 frequently identified in RO permeates (Bereschenko et al., 2008; Stamps et al., 2018);
246 therefore, the identification of bacterial passage mechanisms through RO filters could mainly

247 focus on this bacterial phylum. In this study, Proteobacteria in the RO permeate were further
 248 sub-classified. The class Betaproteobacteria accounted for the majority of bacterial classes in
 249 the RO permeate (84%), followed by the classes Alphaproteobacteria (13%) and
 250 Gammaproteobacteria (0.5%). It is worth noting that *E. Coli* (i.e., a typical bacterial
 251 indicator) belongs to the Gammaproteobacteria.



252
 253 **Fig. 4** Relative abundance of bacteria in the (a) RO feed and (b) permeate. Proteobacteria
 254 were further classified into major classes, orders, and families. “Unk” indicates unknown.

255 Almost all of the Betaproteobacteria found in the RO permeate were represented by the order
 256 Burkholderiales. The Burkholderiales included the families Burkholderiaceae (75%),
 257 Comamonadaceae (5%), and Oxalobacteraceae (3%). Notably, the Burkholderiaceae in
 258 wastewater are known to include the genera *Burkholderia*, *Pandoraea*, *Paraburkholderia*,

259 and *Ralstonia* (Stamps et al., 2018); however, their specific species were not identified in the
260 present study. Three-quarters of the bacteria in the RO permeate belonged to the family
261 Burkholderiaceae, although it accounted for only 0.2% of the bacterial composition in the RO
262 feed. It should be noted that the contamination of microbial DNA that can occur through
263 commonly used DNA extraction kits and other laboratory reagents influences the results of
264 the samples containing a low microbial biomass (Salter et al., 2014); thus, the presented data
265 needs careful assessment. Despite this limitation, the results of this study indicate that the
266 Burkholderiaceae predominantly passed through RO membranes, despite representing a
267 minor proportion of the RO feed bacterial community; however, most other bacterial families
268 were effectively retained by the RO membrane.

269 Bacterial passage mechanisms were further explored in the literature. Burkholderiales (i.e.,
270 85% of the RO permeate bacterial community) are relatively small and rod-shaped bacteria,
271 which are presumably more likely to pass through membranes than other bacterial orders. For
272 example, some species in this family have been reported to exhibit a diameter of 0.4–0.9 μm
273 and a 1.0–2.8 μm length (Gao et al., 2018; Sahin et al., 2011). The Comamonadaceae, which
274 accounted for 5% of the RO permeate bacterial community, include the species *Ramlibacter*
275 *tataouinensis*, which exhibit a diameter of only 0.2 μm and a 3 μm length (Heulin et al.,
276 2003). However, size estimation for nonculturable bacteria is a major challenge; thus, the size
277 of many bacterial species is not well known. Bacteria smaller than 0.1 μm^3 in volume are
278 classified as ultramicrobacteria (Liu et al., 2018; Silbaq, 2009). Moreover, bacteria size can
279 vary greatly depending on the environment and growing conditions (Colwell and Grimes,
280 2000). Therefore, the mechanisms of bacterial passage through RO membranes cannot be
281 solely attributed to differences in bacterial size. Rather, identification of the bacterial species
282 in the RO permeate and their properties (e.g., shape and size) may be instrumental for the
283 development of more effective RO membrane elements for bacterial removal.

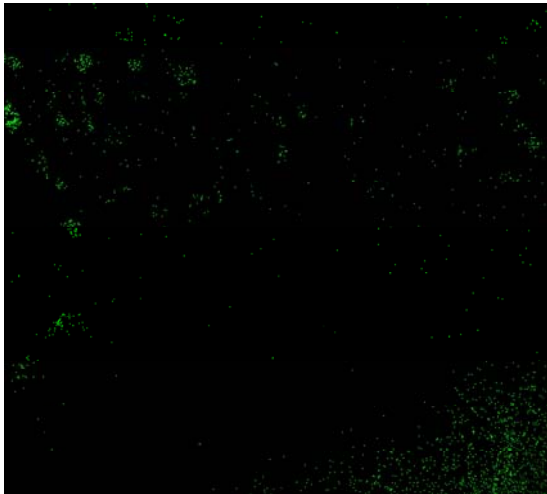
284 3.2 Infiltration routes

285 Evaluations for the passage of bacteria in this study have been conducted based on bacterial
286 concentrations in the RO permeate. Similarly, our previous study (Fujioka and Boivin, 2019)
287 evaluated the removal of bacterial particle by intact and disassembled RO membranes by
288 measuring the concentrations of bacteria-sized surrogates (i.e., FL particles) in the RO feed
289 and permeate, and determined their removal values of 6.8 and 6.0-log, respectively. However,
290 these concentration-based evaluations cannot provide the infiltration routes of bacteria
291 through the RO membranes. Therefore, the specific infiltration routes of bacteria through RO
292 membranes were evaluated using a unique approach—capturing the bacteria-sized surrogates
293 on a 0.2 μm pore size MF filter, which was placed on the permeate side of the intact or
294 disassembled RO membrane (**Fig. 1b**). This study used stable and similarly-sized 0.5 μm FL
295 microspheres as bacteria-sized surrogates to accurately quantify the particle passage without
296 the influence of convective self-aggregation in the RO feed.

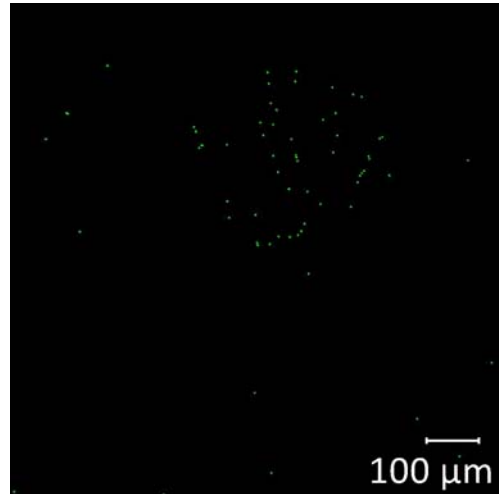
297 When the FL particle solution was treated with the disassembled RO membranes, a
298 substantial number of FL particles (i.e., 532 ± 343 particles/ cm^2 ; $n = 4$) were observed on the
299 track-etched MF membrane (**Fig. 5a**). For example, the captured FL particles formed a spot
300 pattern on the left corner of the filter, and an enlarged representative image demonstrated that
301 these FL particles pass through specific areas of the RO membranes. Contrary to the
302 disassembled RO membranes, the intact RO membranes exhibited very high efficiency for
303 FL particle removal (**Fig. 5b**). A negligible number of FL particles were found to pass
304 through the intact RO membranes (16 ± 1 particles/ cm^2 ; $n = 2$), which was far less than the
305 observed for the disassembled RO membranes. Many FL particles that passed through the
306 disassembled RO membrane gathered in the same places and might have been counted as a
307 single FL particle by the auto-counting software; thus, the measured FL counts are provided
308 only as a qualitative analysis. Moreover, many FL particles appeared to stay behind or inside

309 of the RO membranes without being captured on the MF filter, which may have caused an FL
310 particle count underestimation. Despite these limitations, the major difference in the number
311 of FL particles that passed through the disassembled versus the intact RO membranes
312 indicates that disassembled RO membranes are much more permeable to particles.

(a) Disassembled



(i) Membrane center (11.6 × 10.2 mm)

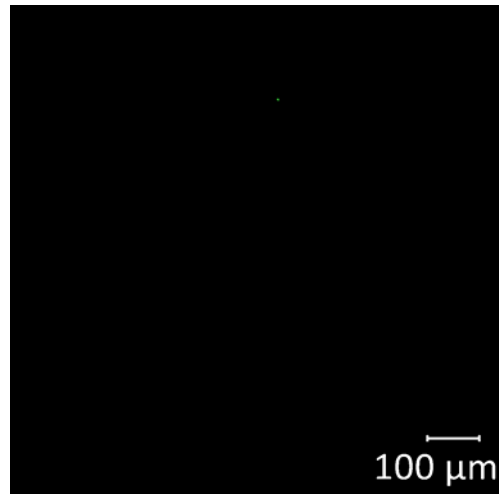


(ii) Enlarged representative image

(b) Intact



(i) Membrane center (11.6 × 10.2 mm)

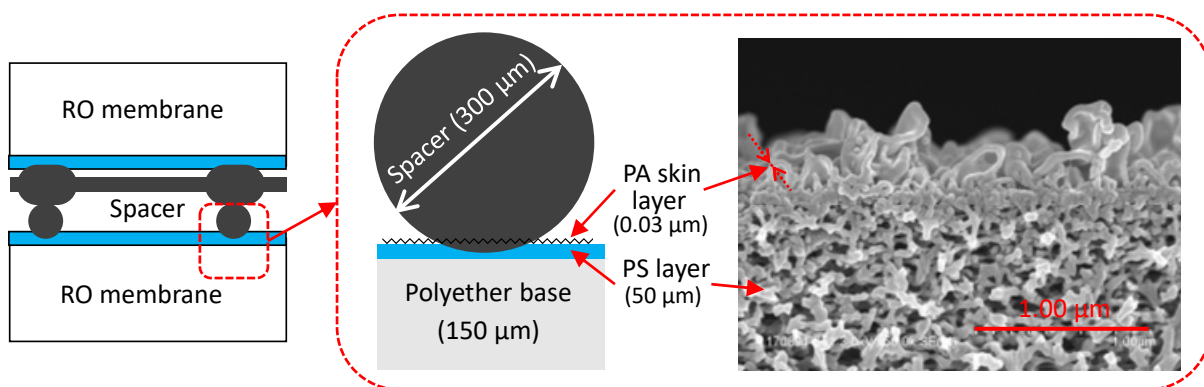


(ii) Enlarged representative image

313 **Fig. 5** Images of fluorescent (FL) particle captured on the track-etched microfiltration (MF)
314 filter after treating the FL particle solution by (a) disassembled or (b) intact reverse osmosis
315 (RO) membranes at a permeate flux of 22 L/m²h and a feed temperature of 25 °C for 120 min.

316 3.3 Implications

317 The passage of FL particles through the disassembled RO membrane sheet occurred likely
318 due to damage caused by an element spacer, as suggested in our previous study (Fujioka and
319 Boivin, 2019). The element spacer is placed between RO membranes in a spiral-wound
320 element to maintain an opening in the RO feed channel (**Fig. 6**). In fact, traces of a spacer
321 were observed on the disassembled RO membrane surface, which is typically observed in
322 disassembled RO membranes provided by many manufacturers. Typical commercial RO
323 membranes have a thin polyamide (PA) skin layer (approximately 0.2–0.4 μm). The skin
324 layer has a hollow interior of crumpled nodules and a ridge-and-valley structure (Fujioka et
325 al., 2018c); thus, the actual thickness of its crumpled film can be as low as 30 nm (i.e., 0.03
326 μm) (Yan et al., 2015).



327
328 **Fig. 6** Schematic cross-sectional images of a feed spacer and reverse osmosis (RO)
329 membrane and a field emission - scanning electron microscope (FE-SEM) cross-sectional
330 images of ESPA2 RO membrane.

331 The diameter of a feed spacer thread is approximately 300 μm , which is far greater than the
332 thickness of the skin layer and UF polysulfone (PS) support layer (**Fig. 6**). Therefore, the skin
333 layer and UF support layer that contacted with the feed spacers can be damaged during the
334 compression of an element assembling process, which may compromise the specific RO
335 membrane regions with a spot pattern, as presented in **Fig. 5**. The compromised regions of
336 the RO membrane surface can allow some small bacterial families in wastewater to

337 predominantly pass through. It should be noted that small constituents in wastewater may
338 influence the passage of these small bacteria during long-term operation, since they may
339 penetrate into the compromised regions and enhance bacterial removal. Because the
340 compromised regions induced by feed spacers can occur throughout the RO membrane sheets,
341 reinforcement of the entire RO membrane surface is required to improve bacterial removal
342 performance. In addition, a future study will explore an approach that visualizes the
343 compromised regions induced by feed spacers.

344 **4 Conclusions**

345 The results of this study using an epifluorescence microscopy and a real-time bacteriological
346 counter indicated continuous passage of bacteria through an RO membrane element. Among
347 bacteria in the UF-treated wastewater, Burkholderiaceae family predominantly passed
348 through RO membrane, although this family only accounted for 0.2% of the RO feed
349 bacterial composition. The results showed that disassembled RO membranes are more
350 permeable to bacterial particles than intact RO membranes, because the thin polyamide skin
351 layer can be damaged by contacting with the RO feed spacers. They are placed between RO
352 membranes throughout the RO membrane element. Therefore, this study suggests that some
353 specific bacterial families in wastewater are particularly capable of passing through the
354 passage located in the entire surface of the RO membrane.

355 **5 Acknowledgement**

356 The authors acknowledge Hydranautics/Nitto for providing an RO membrane element. The
357 authors also acknowledge Azbil Corp. for providing real-time bacteriological monitors.

358 6 References

- 359 Antony, A., Blackbeard, J., Leslie, G., 2012. Removal Efficiency and Integrity Monitoring
360 Techniques for Virus Removal by Membrane Processes. *Crit. Rev. Environ. Sci. Technol.*
361 42(9), 891-933.
- 362 Bereschenko, L.A., Heilig, G.H.J., Nederlof, M.M., van Loosdrecht, M.C.M., Stams, A.J.M.,
363 Euverink, G.J.W., 2008. Molecular characterization of the bacterial communities in the
364 different compartments of a full-scale reverse-osmosis water purification plant. *Appl.*
365 *Environ. Microbiol.* 74(17), 5297-5304.
- 366 Colwell, R.R., Grimes, D.J., 2000. *Nonculturable Microorganisms in the Environment.*
367 Springer.
- 368 Fujioka, T., Boivin, S., 2019. Assessing the passage of particles through polyamide reverse
369 osmosis membranes. *Sep. Purif. Technol.* 226, 8-12.
- 370 Fujioka, T., Hoang, A.T., Aizawa, H., Ashiba, H., Fujimaki, M., Leddy, M., 2018a. Real-
371 Time Online Monitoring for Assessing Removal of Bacteria by Reverse Osmosis. *Environ.*
372 *Sci. Technol. Letters.*
- 373 Fujioka, T., Hoang, A.T., Aizawa, H., Ashiba, H., Fujimaki, M., Leddy, M., 2018b. Real-
374 Time Online Monitoring for Assessing Removal of Bacteria by Reverse Osmosis. *Environ.*
375 *Sci. Technol. Letters* 5(6), 389-393.
- 376 Fujioka, T., Hoang, A.T., Ueyama, T., Nghiem, L.D., 2019a. Integrity of reverse osmosis
377 membrane for removing bacteria: new insight into bacterial passage. *Environ. Sci.: Water*
378 *Res. Technol.* 5(2), 239-245.
- 379 Fujioka, T., Khan, S.J., Poussade, Y., Drewes, J.E., Nghiem, L.D., 2012. *N*-nitrosamine
380 removal by reverse osmosis for indirect potable water reuse – A critical review based on
381 observations from laboratory-, pilot- and full-scale studies. *Sep. Purif. Technol.* 98, 503-515.
- 382 Fujioka, T., Makabe, R., Mori, N., Snyder, S.A., Leddy, M., 2019b. Assessment of online
383 bacterial particle counts for monitoring the performance of reverse osmosis membrane
384 process in potable reuse. *Sci. Total Environ.* 667, 540-544.
- 385 Fujioka, T., O'Rourke, B.E., Michishio, K., Kobayashi, Y., Oshima, N., Kodamatani, H.,
386 Shintani, T., Nghiem, L.D., 2018c. Transport of small and neutral solutes through reverse
387 osmosis membranes: Role of skin layer conformation of the polyamide film. *J. Membr. Sci.*
388 554, 301-308.
- 389 Gao, Z.-h., Zhong, S.-f., Lu, Z.-e., Xiao, S.-y., Qiu, L.-h., 2018. *Paraburkholderia*
390 *caseinilytica* sp. nov., isolated from the pine and broad-leaf mixed forest soil. *Int. J. Syst.*
391 *Evol. Microbiol.* 68(6), 1963-1968.
- 392 Hagen, K., 1998. Removal of particles, bacteria and parasites with ultrafiltration for drinking
393 water treatment. *Desalination* 119(1), 85-91.

- 394 Heulin, T., Barakat, M., Christen, R., Lesourd, M., Sutra, L., De Luca, G., Achouak, W.,
395 2003. *Ramlibacter tataouinensis* gen. nov., sp. nov., and *Ramlibacter henchirensis* sp. nov.,
396 cyst-producing bacteria isolated from subdesert soil in Tunisia. *Int. J. Syst. Evol. Microbiol.*
397 53(2), 589-594.
- 398 Ishida, K.P., Cooper, W.J., 2015. Analysis of parameters affecting process efficiency, energy
399 consumption, and carbon footprint in water reuse. WateReuse Research Foundation,
400 Alexandria, VA.
- 401 Jacangelo, J.G., Aieta, E.M., Cams, K.E., Cummings, E.W., Mallevalle, J., 1989. Assessing
402 Hollow-Fiber Ultrafiltration for Particulate Removal. *Journal - AWWA* 81(11), 68-75.
- 403 Kantor, R.S., Miller, S.E., Nelson, K.L., 2019. The Water Microbiome Through a Pilot Scale
404 Advanced Treatment Facility for Direct Potable Reuse. *Frontiers in Microbiology* 10(993).
- 405 Kitis, M., Lozier, J.C., Kim, J.-H., Mi, B., Mariñas, B.J., 2003. Microbial removal and
406 integrity monitoring of ro and NF Membranes. *Journal - American Water Works Association*
407 95(12), 105-119.
- 408 Kitis, M., Lozier, J.C., Kim, J.H., Mi, B., Mariñas, B.J., 2003. Evaluation of biologic and
409 non-biologic methods for assessing virus removal by and integrity of high pressure
410 membrane systems. *Water Science and Technology: Water Supply* 3(5-6), 81-92.
- 411 Laurent, P., Servais, P., Gatel, D., Randon, G., Bonne, P., Cavard, J., 1999. Microbiological
412 quality: Before and after nanofiltration. *American Water Works Association. Journal* 91(10),
413 62-72.
- 414 Liikanen, R., Miettinen, I., Laukkanen, R., 2003. Selection of NF membrane to improve
415 quality of chemically treated surface water. *Water Res.* 37(4), 864-872.
- 416 Liu, J., Zhao, R., Zhang, J., Zhang, G., Yu, K., Li, X., Li, B., 2018. Occurrence and Fate of
417 Ultramicrobacteria in a Full-Scale Drinking Water Treatment Plant. *Frontiers in*
418 *microbiology* 9, 2922-2922.
- 419 Mi, B., Eaton, C.L., Kim, J.-H., Colvin, C.K., Lozier, J.C., Mariñas, B.J., 2004. Removal of
420 biological and non-biological viral surrogates by spiral-wound reverse osmosis membrane
421 elements with intact and compromised integrity. *Water Res.* 38(18), 3821-3832.
- 422 Miller, S.E., Nelson, K.L., Rodriguez, R.A., 2017. Microbiological Stability in Direct Potable
423 Reuse Systems: Insights from Pilot-Scale Research Using Flow Cytometry and High-
424 Throughput Sequencing. *Proceedings of the Water Environment Federation* 2017(14), 1016-
425 1023.
- 426 Miller, S.E., Rodriguez, R.A., Nelson, K.L., 2020. Removal and growth of microorganisms
427 across treatment and simulated distribution at a pilot-scale direct potable reuse facility.
428 *Environ. Sci.: Water Res. Technol.*
- 429 NWRI, 2013. Examining the Criteria for Direct Potable Reuse, in: Panel, I.A. (Ed.).
430 WateReuse Research Foundation Project 11-02, National Water Research Institute: Fountain
431 Valley, CA, USA.

- 432 Park, S., Hu, J.Y., 2010. Assessment of the extent of bacterial growth in reverse osmosis
433 system for improving drinking water quality. *Journal of Environmental Science and Health,*
434 *Part A* 45(8), 968-977.
- 435 Pecson, B.M., Triolo, S.C., Olivieri, S., Chen, E.C., Pisarenko, A.N., Yang, C.-C., Olivieri,
436 A., Haas, C.N., Trussell, R.S., Trussell, R.R., 2017. Reliability of pathogen control in direct
437 potable reuse: Performance evaluation and QMRA of a full-scale 1 MGD advanced treatment
438 train. *Water Res.* 122, 258-268.
- 439 Pype, M.-L., Lawrence, M.G., Keller, J., Gernjak, W., 2016. Reverse osmosis integrity
440 monitoring in water reuse: The challenge to verify virus removal – A review. *Water Res.* 98,
441 384-395.
- 442 Sahin, N., Tani, A., Kotan, R., Sedláček, I., Kimbara, K., Tamer, A.U., 2011. *Pandoraea*
443 *oxalativorans* sp. nov., *Pandoraea faecigallinarum* sp. nov. and *Pandoraea vervacti* sp. nov.,
444 isolated from oxalate-enriched culture. *Int. J. Syst. Evol. Microbiol.* 61(9), 2247-2253.
- 445 Salter, S.J., Cox, M.J., Turek, E.M., Calus, S.T., Cookson, W.O., Moffatt, M.F., Turner, P.,
446 Parkhill, J., Loman, N.J., Walker, A.W., 2014. Reagent and laboratory contamination can
447 critically impact sequence-based microbiome analyses. *BMC Biol.* 12(1), 87.
- 448 Silbaq, F.S., 2009. Viable ultramicrocells in drinking water. *J. Appl. Microbiol.* 106(1), 106-
449 117.
- 450 Stamps, B.W., Leddy, M.B., Plumlee, M.H., Hasan, N.A., Colwell, R.R., Spear, J.R., 2018.
451 Characterization of the Microbiome at the World's Largest Potable Water Reuse Facility.
452 *Frontiers in Microbiology* 9(2435).
- 453 Tchobanoglous, G., Cotruvo, J., Crook, J., McDonald, E., Olivieri, A., Salveson, A., Trussell,
454 R.S., 2015. Framework for direct potable reuse. *WaterReuse Association, American Water*
455 *Works Association, Water Environment Federation, National Water Research Institute,*
456 *Alexandria, VA.*
- 457 WHO, 2017. Potable reuse: guidance for producing safe drinking-water. *World Health*
458 *Organization, Geneva.*
- 459 Wijmans, J.G., Baker, R.W., 1995. The solution-diffusion model: a review. *J. Membr. Sci.*
460 107(1-2), 1-21.
- 461 Yan, H., Miao, X., Xu, J., Pan, G., Zhang, Y., Shi, Y., Guo, M., Liu, Y., 2015. The porous
462 structure of the fully-aromatic polyamide film in reverse osmosis membranes. *J. Membr. Sci.*
463 475(0), 504-510.
- 464 Zhang, J., Cran, M., Northcott, K., Packer, M., Duke, M., Milne, N., Scales, P., Knight, A.,
465 Gray, S.R., 2016. Assessment of pressure decay test for RO protozoa removal validation in
466 remote operations. *Desalination* 386, 19-24.

467